

## **Silica Fume Modified Cement-Based Mortar Exposed to High Temperatures: Residual Strengths and Microstructure**

**Shahad Jafeer Albeer<sup>1,\*</sup>, Maan Salman Hassan<sup>2</sup>**

<sup>1</sup>Department of Civil Engineering, College of Engineering, University of Baghdad, Baghdad, Iraq

<sup>2</sup>Department of Civil Engineering, University of Technology, Baghdad, Iraq

[shahad.kamel2001m@coeng.uobaghdad.edu.iq](mailto:shahad.kamel2001m@coeng.uobaghdad.edu.iq)<sup>1</sup>, [40018@uotechnology.edu.iq](mailto:40018@uotechnology.edu.iq)<sup>2</sup>

### **ABSTRACT**

Several previous investigations and studies utilized silica fume (SF) or (micro silica) particles as supplementary cementitious material added as a substitute to cement-based mortars and their effect on the overall properties, especially on physical properties, strength properties, and mechanical properties. This study investigated the impact of the inclusion of silica fume (SF) particles on the residual compressive strengths and microstructure properties of cement-based mortars exposed to severe conditions of elevated temperatures. The prepared specimens were tested and subjected to 25, 250, 450, 600, and 900 °C. Their residual compressive strengths and microstructure were evaluated and compared with control samples (CS) subjected to similar conditions (the same temperature category). The outcomes indicated that including silica fume particles in mortar mixtures lowered the amount and width of microcracks, upgraded the mass-loss performance, lowered crystalline calcium hydroxide, and reinforced the cement paste, which explained the improvement in residual mechanical strengths.

**Keywords:** Elevated Temperatures, Silica Fume, Cement-Based Mortars.

---

\*Corresponding author

Peer review under the responsibility of University of Baghdad.

<https://doi.org/10.31026/j.eng.2023.07.02>

This is an open access article under the CC BY 4 license (<http://creativecommons.org/licenses/by/4.0/>).

Article received: 10/08/2022

Article accepted: 09/10/2022

Article published: 01/07/2023



## مونة السمنت المحسنة بغبار السيليكا والمعرضة لدرجات حرارة عالية: الاجهادات المتبقية والتركيب المايكروي

شهد جعفر البير<sup>1\*</sup>، معن سلمان حسن<sup>2</sup>

<sup>1</sup>قسم الهندسة المدنية، كلية الهندسة، جامعة بغداد، بغداد، العراق

<sup>2</sup>قسم الهندسة المدنية، جامعة التكنولوجيا، بغداد، العراق

### الخلاصة

اهتمت العديد من البحوث السابقة المتعلقة باستخدام حبيبات غبار السليكا كمادة مكملة في مونة السمنت وتأثيرها على الصفات الفيزيائية، المقاومة والخواص الميكانيكية. في هذه الدراسة، تم فحص تأثير تضمين غبار السيليكا على مقاومة الانضغاط المتبقية والتركيب المجهرى لمونة السمنت بعد التعرض لدرجات حرارة عالية. تم تعويض العينات المفحوصة لدرجات حرارة 25 سيليزية، 250 سيليزية، 450 سيليزية، 600 سيليزية، 900 سيليزية. تم تقييم مقاومة الانضغاط المتبقية والتركيب المجهرى وقورنت مع العينات المرجعية التي تعرضت لدرجات حرارة مشابهة. اظهرت النتائج ان تضمين حبيبات غبار السيليكا الى الخلطة الاسمنتية قللت كمية وعرض الشقوق المايكروية، حسنت من اداء المادة الناتجة من ناحية فقدان الكتلة، قللت من كمية هيدروكسيد الكالسيوم المتبلور وقوت معجون الاسمنت الذي يفسر سبب التحسن في المقاومة الميكانيكية المتبقية.

**الكلمات الرئيسية:** درجات الحرارة العالية، غبار السيليكا، مونة الاسمنت.

### 1. INTRODUCTION

Cement-based composites are commonly used as main structural material in buildings and other structures owing to their many benefits, such as their simplicity of production and non-combustibility properties, as well as their strength and durability characteristics. When used in buildings, cement-based mortar products must satisfy international code requirements for fire resistance and elevated temperature safety. Therefore, specific appropriate fire resistance provisions and measures for concrete structures are an important aspect in the design stage (**European Committee for Standardization, 2004; ACI 318R-14, 2014; Kodur, 2014; Joint ACI/TMS Committee 216.1-14, 2019; Ibrahim and Allawi, 2023**).

Many pozzolanic materials have been used as alternatives for cement to increase its durability and high-temperature resistance and increase the sustainability of the products made. (**Garg et al., 2020; Khalid and Abbas, 2023**) used silica fume as an alternative to cement. (**Mohammed et al., 2022**) used alkali-activated natural pozzolans as cement alternatives, etc. In the current study, silica fume has been used as an active pozzolan to investigate its effect on the properties of cement mortar, mainly compressive strength and high-temperature resistance. The creation of silicon or silicon alloys generates micro-silica (MS), also known as silica fume (SF) (**Swamy, 1986; Bolhassani and Samani, 2014; Hassan, 2017**). Particle size is typically between 0.1 and 0.5  $\mu\text{m}$ , and its nitrogen BET



surface area is about 20,000 m<sup>2</sup> /kg (Swamy, 1986). It comprises silica with high purity (>80%) in an amorphous state. Silica fume has grown in popularity over the years to be among the most widely utilized additional cementitious materials in manufacturing high-strength concrete and high-performance concrete (Abdulkareem et al., 2016; Wu and Khayat, 2016). To increase the longevity of concrete buildings, it is common practice to use SF as a supplemental cementitious material. (Mardani-Aghabaglou et al., 2014) examined the efficacy of fly ash, metakaolin, and SF in improving mortar's mechanical characteristics and durability and concluded that SF was the most successful of the supplemental cementitious materials studied.

(Garg et al., 2020) investigated the strength and microstructure of cement mortars with the incorporation of SF. The findings showed that the optimized usage of SF can give beneficial effects to improve the new properties and strength with dense microstructure. Self-compacting concrete was produced by (Gesog et al., 2009) using binary, ternary, and quaternary mixes of cement, fly ash, slag, and SF, respectively. The results showed that the cement, slag, and SF ternary blend had the highest durability. To estimate the long-term chloride diffusion in concrete using SF, Farahani et al. used SF in the production of marine concrete.

Numerous research studies examine how increasing the temperature of cement-based composites changes their strength and microstructure properties. (Kodur, 2014) illustrated that significant changes occur to the concrete after exposure to high temperatures. (Alani et al., 2020) found that high temperatures affect cement mortar's physical, chemical, and mechanical properties. (Moghadam and Izadifard, 2020) demonstrated that temperatures above 400 °C cause a significant loss of mechanical properties in cement mortar. Increases in temperature cause or contribute to changes in the microstructure of cement-based materials, mainly caused by dehydration. (Kodur, 2014; Li et al., 2018; Alani et al., 2020) found that at temperatures of 105 °C or above, CSH gel desiccates. This is proof that the phenomena are not fully characterized or understood. Furthermore, strain incompatibilities of their elements are of concern in hot mortars and concrete (Farzadnia et al., 2013). In contrast to cement paste, which continues to stretch up to 150 °C and then collapses beyond that temperature (Kodur, 2014), aggregates always expand when heated. The disappearance of encapsulated water is to blame for the resulting shrinkage, which in turn leads to the formation of microcracks that may alter the material's porosity and permeability. Mostly, residual characteristics data infer how temperature affects cementitious material properties (Ibrahim et al., 2014; Alani, 2020)

This paper focuses on using silica fume to improve the high-temperature resistance of cement-based mortars. Its goal is to create a modified high-temperature resistance mortar by adding silica fume and then study the effect of high temperature on the mortars produced. The output of this study is expected to provide a better understanding of the behavior of cement-based materials that contain silica fume and their behavior after exposure to extreme temperatures.

## 2. MATERIALS AND METHOD

### 2.1 Materials

This study used Ordinary Portland Cement (OPC) produced at the Kubaisa cement factory, conforming to ASTM C150 and Iraqi specification No.5/2019, as shown in **Table 1**. The



chemical composition and physical properties of the used cement (obtained from the Research and Development Division of Kubaisa Factory) are presented in **Table 2**.

**Table 1.** The physical test results of the used cement.

Physical Requirements	Test Result	Iraqi Specification NO.5 1984
Specific surface area blain (m <sup>2</sup> /kg)	281	≥ 230
Setting time-vacant apparatus		
Initial setting (minutes)	111	≥45
Final setting (minutes)	298	≤600
Compressive strength		
3 days (MPa)	15.7	≥15
7 days (MPa)	24.2	≥23

**Table 2.** Chemical analysis and physical properties of cement.

Chemical analysis (% by weight)	
CaO	54.28
SiO <sub>2</sub>	24.15
Al <sub>2</sub> O <sub>3</sub>	4.04
Fe <sub>2</sub> O <sub>3</sub>	3.92
MgO	4.6
SO <sub>3</sub>	1.99
Loss on ignition	3.37
Insoluble Residue	1.10
C <sub>3</sub> S	42
C <sub>2</sub> S	30
C <sub>3</sub> A	3.95
C <sub>4</sub> AF	11.89

Standard sand was selected as a fine aggregate to prepare mortar mixtures. Standard sand was intended to reduce the variations in the results that affect mortar more than concrete. Its specific gravity, silica content, SO<sub>3</sub> content, and maximum particle size were 2.6, 0.9%, 90.11%, and 0.18 mm, respectively. Natural silica sand, consisting almost entirely of naturally round grains of semi-pure quartz, aggregate classification, and physical properties are explained in **Tables 3, 4, and 5**. They all fulfill the requirements of (ASTMC778, 2013) and (IQS No. 2080, 1998), respectively.

**Table 3.** Specifications of the used sand according to ASTM C778, 2013.

Sieve size (mm)	Passing by weight (%)	Limit of Passing percentage according to ASTM Specification %
1.18 (No. 16)	100	100
850 (No. 20)	99.5	85 to 100
600 (No. 30)	4	0 to 5

**Table 4.** Specifications of the used sand according to Iraqi specifications (IQS No. 2080/1998).

Sieve size	Passing by weight	Limit of Passing percentage according to IQS No.2080/1998 Specification %
850 (No. 20)	99.5	98 min
600 $\mu\text{m}$ (No. 30)	4	10 max

\*The tests were carried out by the National Center for Geological Survey and Mines.

**Table 5.** Properties of the sand used in this work.

Physical properties	Test result	Limit of Iraqi specification No.45/1984
Specific gravity	2.6	-
Absorption %	1	-
Sulfate content %	0.35	0.5%

\*The National Center for Geological Survey and Mines conducted the tests.

Non-absorbent monofilament polypropylene (PP) fibers (specific gravity 0.9 g/cc) with an average fiber length of 6 mm and diameter of 0.18 mm were used. **Fig. 1** (left side) shows the used PP fibers. It could withstand temperatures above 100 °C for brief durations without melting, with a melting point of 165 °C.

Condensed SF (**Fig. 1** right side) was used as a mineral admixture, which works physically to optimize the mortar mixtures' particle packing and chemically as a highly reactive pozzolan. Its specific gravity and bulk density were 2.3 g/cc and 600 kg/m<sup>3</sup>, respectively. **Table 6.** shows the chemical composition of the used SF.

**Table 6.** Chemical composition of SF.

Compound	SiO <sub>2</sub>	Al <sub>2</sub> O <sub>3</sub>	Fe <sub>2</sub> O <sub>3</sub>	CaO	MgO	SO <sub>3</sub>
Weight %	81.40	4.47	1.40	0.82	1.48	1.30

**Figure 1.** Left side: Polypropylene fibers, and right side: SF powder.

## 2.2 Preparing Mortar for High Temperatures Exposure

The ASTM C305 standard specifies the use of 2% SF as a cement substitute by weight in the production of mortars. Binder ingredients (cement and SF) were blended by hand for 5 minutes. Binder-to-sand weight ratios 1:2.75 were utilized (ASTM C109, 2010; ASTM C305, 2011; Alani et al., 2020a; Alani et al., 2020b), as was a constant water-to-binder ratio (w/b) of 0.45. The mortar flow was maintained at 110 mm 5% throughout the trial by varying the naphthalene sulfonate-based superplasticizer (SP) proportion according to ASTM C494 (Type F). The fresh mortar flow was evaluated using (ASTM C1437, 2020), and the results are shown in Fig. 2. The spalling effect caused by high temperatures was reduced by including PP fibers at a volume fraction of 0.1% or higher (0.04% by weight). The relative amounts of each component in the blend are shown in Table 7. Test samples were prepared into cubes measuring 50 mm on all sides in Fig. 3. Each sample was cast, then stored in molds at 100% relative humidity (RH) for 1 day before being gotten out of the molds and cured in lime-saturated water at  $23\pm 2$  °C until the age of testing (28 or 90 days).

Table 7. Mix proportions of the prepared samples.

Component	Quantity CS	Quantity SFS
Binder (cement + SF)	(1+0) =1	(0.98+0.02) =1
Sand (g)	2.75	2.75
w/b ratio	0.45	0.45
SF (% by wt. of cement)	0	2
SP (% by wt. of cement)	1.8	2
PP (% by wt.)	0.04	0.04



Figure 2. Flow test of mortar.



Figure 3. Mortar samples after casting.

Wet samples from each combination were dried using a towel before testing (Ibrahim et al., 2014). Afterward, they were heated to 250 °C, 450 °C, 600 °C, and 900 °C for 2 hours at a heating rate of 10 °C/min in Fig. 4) and eventually cooled to ambient temperature (25 °C) within the furnace at about the same pace (Chen et al., 2009; Seleem et al., 2011; Morsy et al., 2012; Irshidat and Al-Saleh, 2018; Abayou et al., 2019; Alani et al., 2020b). The following day, the samples were prepared for elevated temperatures. For this reason, a



digital screen-connected furnace (Carbolite, UK) was used, with the desired temperature and measurement duration regulated by a pre-programmed test configuration. To guarantee that the whole test sample attained thermal steady-state and equilibrium conditions, the temperature was raised to the desired level and held there for 2 hours (Morsy et al., 2012; Kodur, 2014; Irshidat and Al-Salih, 2018).



**Figure 4.** The furnace used and samples inside it.

The loss of water by evaporation is a major factor in the loss of mass that occurs in cement-based materials when heated to high temperatures (Kjellsen et al., 2003). Cement mortar samples were weighed before and after being heated under controlled circumstances. The difference between the two weights was recorded as the mass loss.

### 2.3 Testing Methods

Three samples were taken from each heating condition, plus a control (unheated) sample (CS), and subjected to compression testing following ASTM C109. Fig. 5 shows some of the sample's test setup using 2000 KN. Electronic Concrete Equipment (ELE) is a brand of concrete compression equipment. Samples were analyzed at 28 and 90 days at Bodour Residential Complex Company.



**Figure 5.** Compression test set-up.

The fractured surface of the sample was detected before and after being heated to various temperatures using a scanning electron microscope at voltages of up to 30 kV at an operating distance of 1–12 mm, using a tungsten source. The humidity was avoided



throughout the sample processing phase by heating and storing the fractured samples in a desiccator (a few hours). Preparation for scanning electron microscopy (SEM) imaging included drying the samples in an oven and coating them with gold with estimated dimensions of 10\*10\*10 mm (Kjellsen et al., 2003; Hassan, 2018; Kattoof et al., 2022).

### 3. RESULTS AND DISCUSSION

#### 3.1 Compressive Strength

The residual strengths of CS and SF samples cured for 28 and 90 days, tested at 25 °C, and tested after exposure to elevated temperatures (250, 450, 600, and 900 °C), were presented in Fig. 6. Results showed a decrease in residual compressive strength for the samples cured for 28 days in Fig. 6(a) as the temperature increases. This is expected behavior because elevated temperatures tend to deteriorate physical, chemical, and mechanical properties (Lea, 1920; Lea and Stradling, 1922; Taylor, 1964; Orchard, 1979; Khoury, 1992; Neville, 1995).

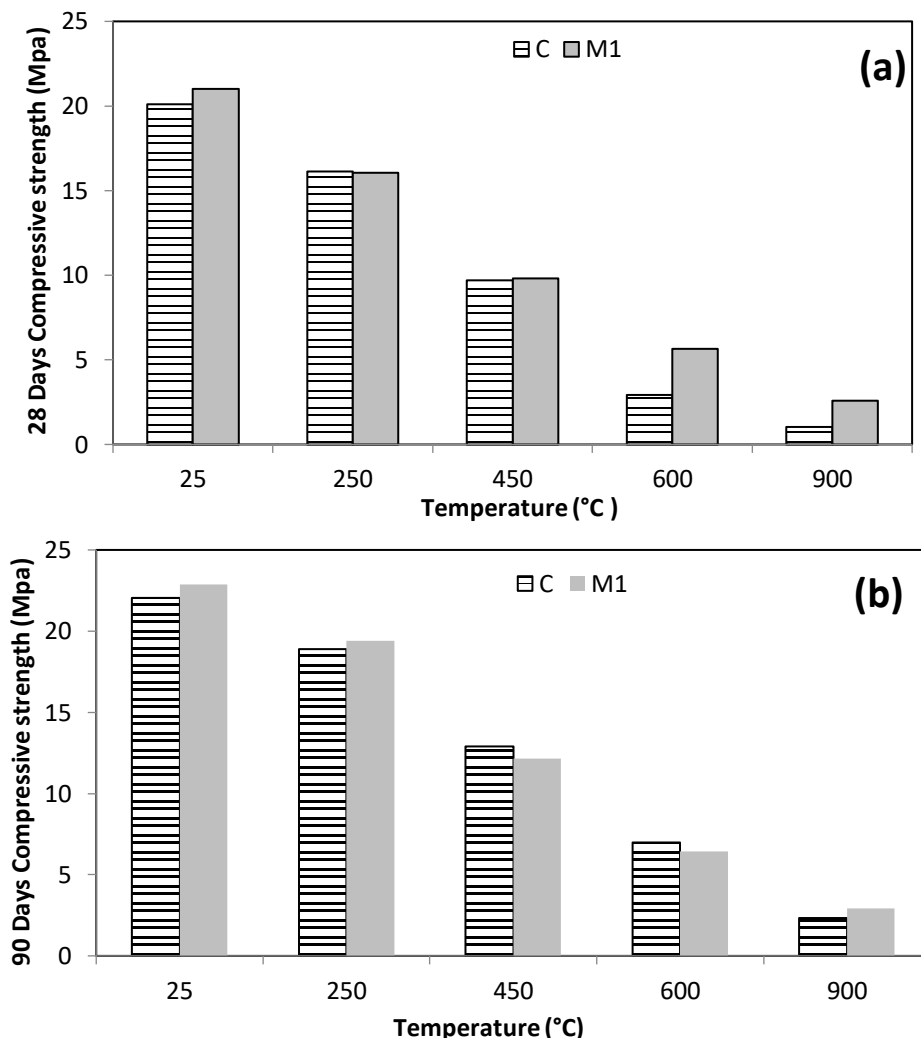


Figure 6. The compressive strengths of CS and SFS-modified cement mortar cured for (a) 28 days and (b) 90 days at different temperatures (25, 250, 450, 600, and 900) °C.





A slight increase in residual compressive strength for the micro silica sample above the CS at temperatures of 25, 250, and 450 °C may be attributed to the effect of high temperatures. In this range of temperatures, the cement paste undergoes accelerated hydration reactions and consumption of the trapped water and other unreacted cementitious ingredients (**Escalante-Garcia and Sharp, 1998**). While in the temperature range from 600 to 900 °C, SFS displays higher residual compressive strength compared to CS due to the reinforcement effect of the microspheres of silica, which tend to withstand the formation of micro and macro cracks and also reduce water loss and the fragile boundary layer between aggregate and paste. Compared to CS, mortar made with silica fume cement will have much less permeability due to the micro-filler effect that strengthens the paste-to-aggregate connection. Accelerated strength and durability in fresh mortars are a result of the silica reaction (**Sharma et al., 2014**). The same behavior for the samples cured for 90 days in **Fig. 6(b)** was noticed but with higher residual compressive strength. In the 25 and 250 °C, SFS showed slightly higher residual compressive strength than CS. However, in the range of 450 and 600 °C, CS revealed to some extent, comparable residual compressive strengths (**Khaloo et al., 2011; Bolhassani and Samani, 2014**).

**Fig. 7** represents a graph of the percentage difference in compression strengths between the samples subjected to high temperatures and untreated mortar samples after 28 days. Both 28-day and 90-day compressive strengths of cement mortar mixes modified by SF are slightly higher than those of CS. On application of high temperatures (250, 450, 600, and 900°C) to the CS, the decrease in the percentage of the compressive strength value was 19.88%, 51.88%, 85.4%, 94.8 respectively at 28 days, concerning CS at room temperature (25 °C). However, on adding 2% SF to the cement mortar, the decrease in the percentage of the compressive strength value was 23.61%, 53.33%, 73.14%, and 87.61%, respectively, at 28 days, with respect to SFS at room temperature (25 °C).

For the samples cured for 90 days, the percentage of change in compressive strength of CS was lower than that of SFS. It was noticed that there was a slight effect on the percentage difference in compression strengths of 2% wt. of SF due to the low percentage of substitution of SF. So, to achieve the desired effect, it is necessary to explore the effects of adding higher percentages of SF. The effect of SF incorporation on the compressive strength of cement mortar has been discussed in many publications. The major influence of SF on the compressive strength of cement mortar is increasing compressive strength (**Temiz and Karakec, 2002; Khaloo et al., 2011; Güneyisi et al., 2012; Sharma et al., 2014; Bolhassani and Samani, 2014; Li et al., 2017; Azimi-pour and Eskandari-Naddaf, 2018; Janca et al., 2019**).

**Fig. 7** also shows that the percentage of changes in compressive strength was more pronounced at 90 days than at 28 days. A possible explanation for this behavior is that the pozzolanic activity of SF increased with time (90-day age). More CSH gels were produced, causing further densification and better strength for the cement-based matrix.

### 3.2 Scanning Electron Microscopy (SEM)

**Fig. 8** shows the SEM of CS and SFS at room temperature cured for 28 days. It is noticed that the rich internal structure is represented by the rod-like structure, which is CSH (**Mehta and Monteiro, 2014**). The small crystals, which resemble  $\text{Ca(OH)}_2$  (**Kim et al., 2013**), as well as the small dark areas filled with trapped water, are more noticeable in the CS (left side), where the SF replaces it, so it appears less in the SFS sample (right side) (**Fridland and Rosado, 2003**).

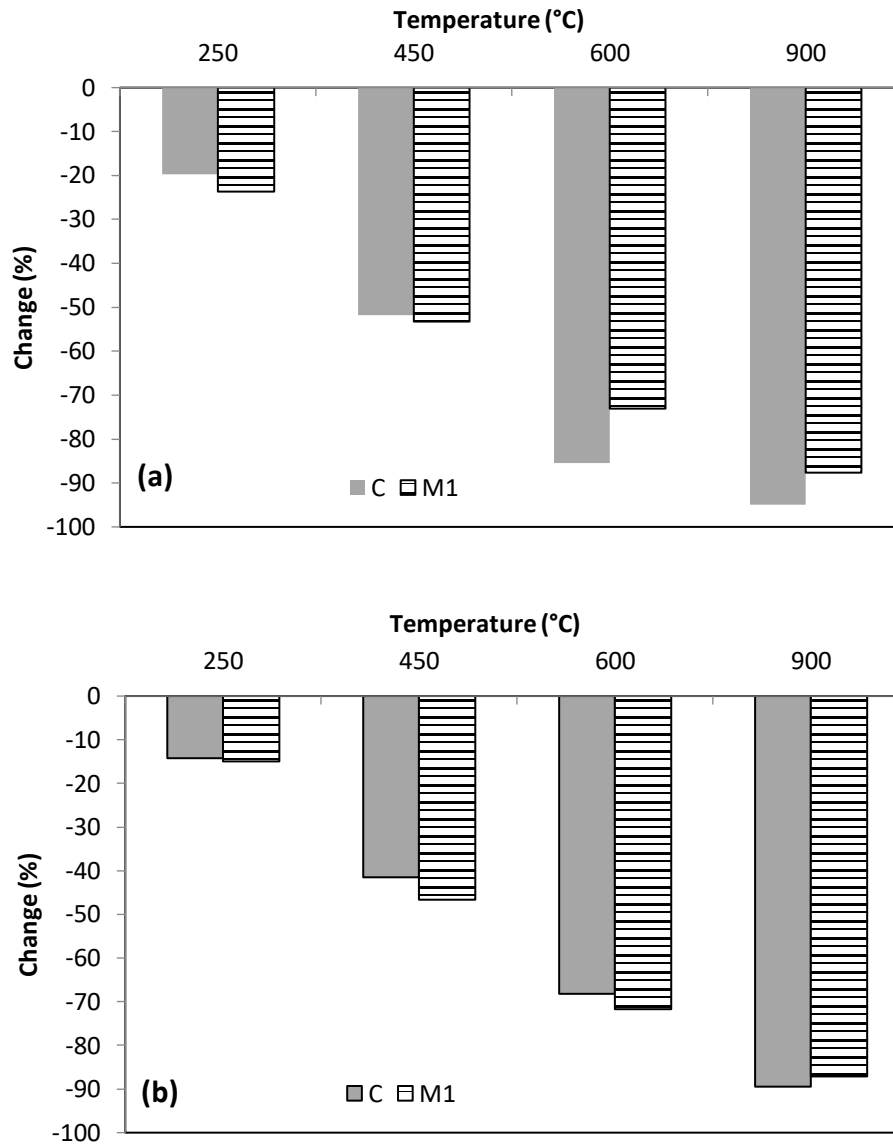


**Figure 7.** Percentage of change in compressive strength of cement mortar in different temperatures (250, 450, 600, and 900) °C for (a) 28 days and (b) 90 days ages of cured samples.

**Fig. 9** represents the CS and SFS after exposure to 250 °C. A magnification of 5  $\mu\text{m}$  was taken to compare the two results easily. It can be noticed that the unreacted particles of cement were along the surface of CS (left side); also, it is obvious that the surface of the sample was covered with crystals in a layered form, and no pores appeared. This could be due to the accelerated hydration reaction of the constituents with the trapped water, and the resulting crystals filled most possible places, forming this layered structure (**Knapen and Gemert, 2009**). With the SFS (right side), stacked spheres of remaining SF appeared to cover the formed crystals. Some micro-cracks could lead to more macro and micro-cracks in more severe conditions.

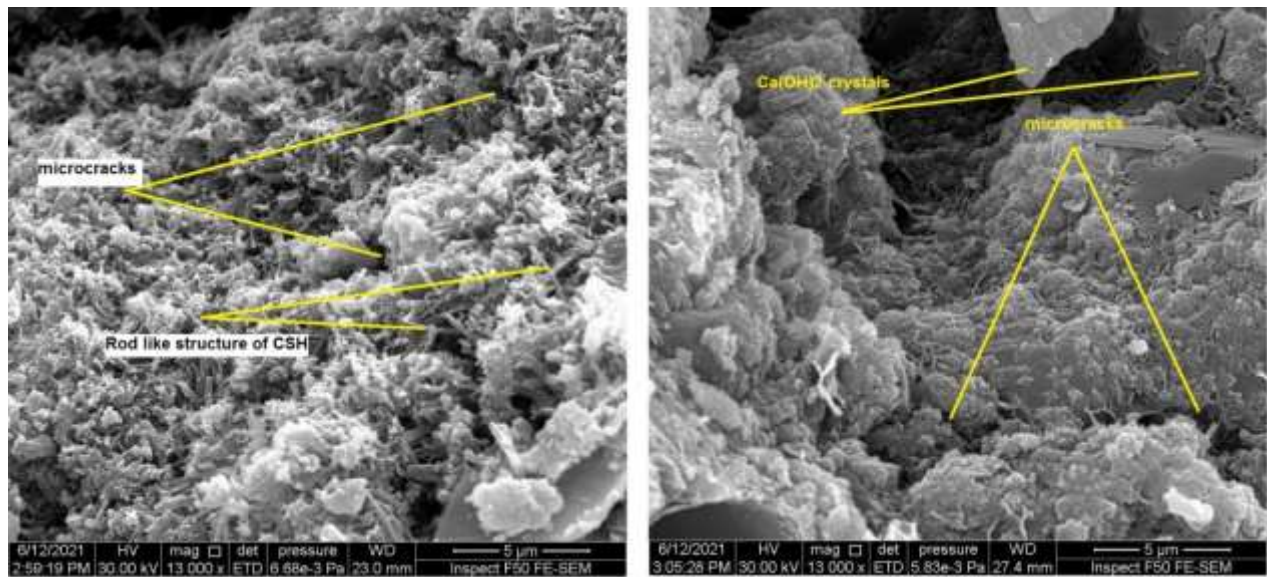


Figure 8. (left side) CS and (right side) SFS at 25 °C.

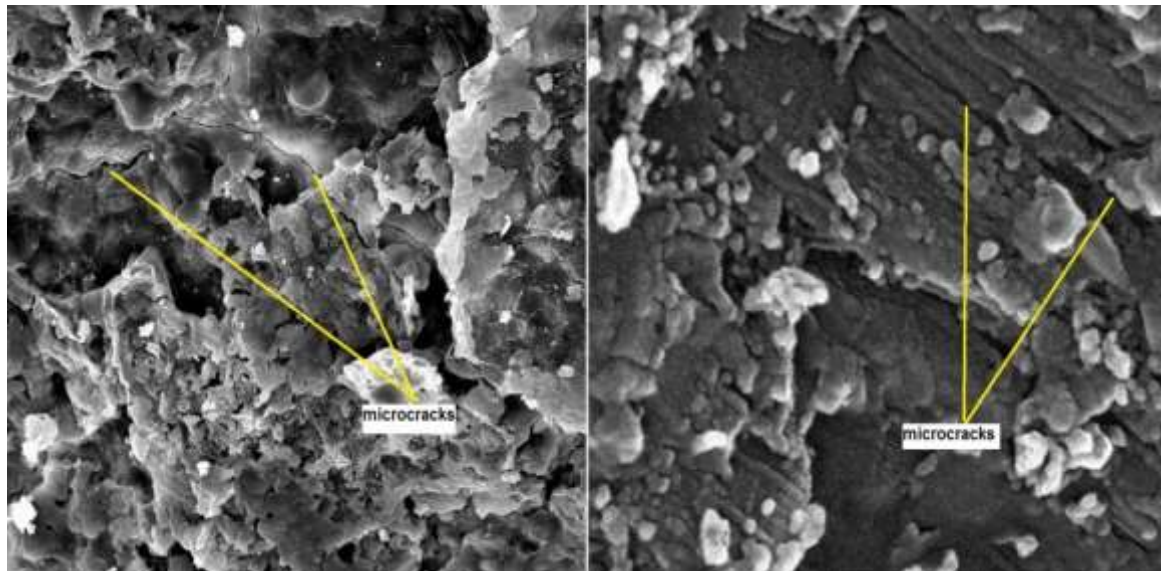
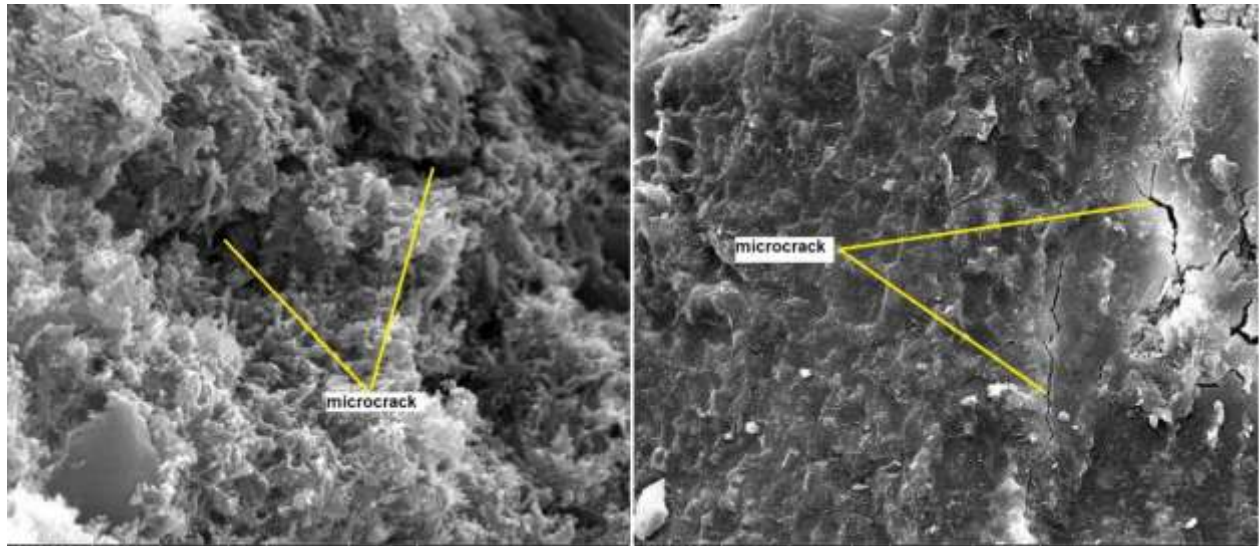


Figure 9. (left side) CS and (right side) SFS at 250 °C.

**Fig. 10** shows the CS and SFS at 900 °C. This high temperature is mostly responsible for the deterioration of the cement paste, as seen in the CS (left side), where the rod-like network of CSH decays and the crystals of  $\text{Ca(OH)}_2$  decompose with more apparent cracks and pores (Castellotea et al., 2004; Menendez et al., 2012). While on the other side (right side), most of the crystals and CSH have been damaged, and only the small spheres of SF appear from under the degraded cement paste. Also, on both sides of **Fig. 10**, it was seen that the deep cracks appeared more clearly, and this is the cause of the lower mechanical properties.



**Figure 10.** (left side) CS and (right side) SFS at 900 °C.

#### 4. CONCLUSIONS

This study assessed the effects of silica fume to improve the high-temperature resistance of cement-based mortars. Based on the results of the experimental program of this study, the following conclusions are drawn:

1. Compared with mortars without SF, incorporating SF into cement mortar showed an increase in compressive strength for 28 and 90 days of curing after exposure to elevated temperatures (250, 450, 600, and 900 °C).
2. Incorporating higher dosages of SF could enhance the residual compressive strength and stability, particularly at later ages. This behavior may be interpreted due to SF's reactivity, which induces more pozzolanic reactions.
3. SEM images revealed the presence of CSH and  $\text{Ca}(\text{OH})_2$  (portlandite), represented by rod-like structures and layered crystals, respectively. The decomposition of these hydration products increases as the temperature increases.
4. According to the results of the microstructural analysis, the mortar matrix retained its structural stability even after being heated to 250 °C when cement was replaced with SF.
5. At higher temperatures (450, 600, and 900 °C), there was cracking, severe deterioration, and eventually collapse of the material, with 94% and 87% percentage reductions in the compressive strength of CS and SFS, respectively. This proves that incorporating SF could significantly reduce the damaging effects of fire on cement mortar if used in the proper proportions.

The output of this study would be useful for engineers and designers interested in providing protection barriers to minimize the fire effects on structures and buildings to confirm international standards.



**REFERENCES**

ACI-318, 2014. Building Code Requirements for Structural Concrete (ACI 318-14) and Commentary.

Abayou, A., Yasien, A.M. and Bassuoni, M.T., 2019. Properties of nanosilica-modified concrete cast and cured under cyclic freezing/low temperatures. *Advances in Civil Engineering Materials*, 8(3), pp.287-306. [Doi:10.1520/ACEM20190013](https://doi.org/10.1520/ACEM20190013).

Abdulkareem, R.T., Hassan, M.S. and Gorgis, I.N., 2016. Effect of steel fibers, polypropylene fibers and/or nanosilica on mechanical properties of self-consolidating concrete. *Engineering and Technology Journal*, 34(3 Part A), pp.527-538. [Doi: 10.30684/etj.34.3A.8](https://doi.org/10.30684/etj.34.3A.8)

Alani, S., Hassan, M.S., Jaber, A.A. and Ali, I.M., 2020. Effects of elevated temperatures on strength and microstructure of mortar containing nano-calcined montmorillonite clay. *Construction and Building Materials*, 263, p.120895. [Doi:10.1016/j.conbuildmat.2020.120895](https://doi.org/10.1016/j.conbuildmat.2020.120895).

Alani, S.S., Hassan, M.S. and Jaber, A.A., 2020, February. Residual strength and degradation of cement mortar containing polypropylene fibers at elevated temperature. In *IOP Conference Series: Materials Science and Engineering* (Vol. 737, No. 1, p. 012065). IOP Publishing. [Doi:10.1088/1757-899X/737/1/012065](https://doi.org/10.1088/1757-899X/737/1/012065).

ASTM C109, 2010. Standard Test Method for Compressive Strength of Hydraulic Cement Mortars, ASTM International.

ASTM C1437, 2020. Standard Test Method for Flow of Hydraulic Cement Mortar. ASTM International.

ASTM C305, 2011. Standard Practice for Mechanical Mixing of Hydraulic Cement Pastes and Mortars of Plastic Consistency. ASTM International.

Azimi-Pour, M., Eskandari-Naddaf, H., 2018. ANN and GEP prediction for simultaneous effect of nano and micro silica on the compressive and flexural strength of cement mortar. *Construction and Building Materials*, 189, pp.978–992. [Doi:10.1016/j.conbuildmat.2018.09.031](https://doi.org/10.1016/j.conbuildmat.2018.09.031).

Bolhassani, M. and Samani, M., 2015. Effect of type, size, and dosage of nanosilica and microsilica on properties of cement paste and mortar. *ACI Materials Journal*, 112(2), pp.1-7.

Castellote, M., Alonso, C., Andrade, C., Turrillas, X. and Campo, J., 2004. Composition and microstructural changes of cement pastes upon heating, as studied by neutron diffraction. *Cement and concrete research*, 34(9), pp.1633-1644. [Doi:10.1016/S0008-8846\(03\)00229-1](https://doi.org/10.1016/S0008-8846(03)00229-1).

Chen, B., Li, C. and Chen, L., 2009. Experimental study of mechanical properties of normal-strength concrete exposed to high temperatures at an early age. *Fire Safety Journal*, 44(7), pp.997-1002. [Doi:10.1016/j.firesaf.2009.06.007](https://doi.org/10.1016/j.firesaf.2009.06.007).

Escalante-Garcia, J.I. and Sharp, J.H., 1998. Effect of temperature on the hydration of the main clinker phases in Portland cements: Part I, neat cements. *Cement and concrete research*, 28(9), pp.1245-1257. [Doi: 10.1016/S0008-8846\(98\)00115-X](https://doi.org/10.1016/S0008-8846(98)00115-X)

European Committee for Standardization, EN, 1992-1-2: design of concrete structures. Part 1-2: general rules—structural fire design, Brussels, Belgium.



Farzadnia, N., Ali, A.A.A. and Demirboga, R., 2013. Characterization of high strength mortars with nano alumina at elevated temperatures. *Cement and Concrete Research*, 54, pp.43-54. [Doi:10.1016/j.cemconres.2013.08.003](https://doi.org/10.1016/j.cemconres.2013.08.003)

Fridland, M. and Rosado, R., 2003. Mineral trioxide aggregate (MTA) solubility and porosity with different water-to-powder ratios. *Journal of endodontics*, 29(12), pp.814-817. [Doi:10.1097/00004770-200312000-00007](https://doi.org/10.1097/00004770-200312000-00007)

Gesoğlu, M., Güneyisi, E. and Özbay, E., 2009. Properties of self-compacting concretes made with binary, ternary, and quaternary cementitious blends of fly ash, blast furnace slag, and silica fume. *Construction and building materials*, 23(5), pp.1847-1854. [Doi:10.1016/j.conbuildmat.2008.09.015](https://doi.org/10.1016/j.conbuildmat.2008.09.015).

Güneyisi, E., Gesoğlu, M., Karaoğlu, S. and Mermerdaş, K., 2012. Strength, permeability and shrinkage cracking of silica fume and metakaolin concretes. *Construction and Building Materials*, 34, pp.120-130. [Doi:10.1016/j.conbuildmat.2012.02.017](https://doi.org/10.1016/j.conbuildmat.2012.02.017)

Garg, R., Garg, R., Bansal, M. and Aggarwal, Y., 2021. Experimental study on strength and microstructure of mortar in presence of micro and nano-silica. *Materials Today: Proceedings*, 43, pp.769-777. [Doi:10.1016/j.matpr.2020.06.167](https://doi.org/10.1016/j.matpr.2020.06.167).

Hassan, M.S., Gorgis, I. and Jaber, A., 2017. Fresh and hardened properties of nanosilica and microsilica contained self-consolidating concretes. *ARPN J Eng Appl Sci*, 12, pp.5140-5153.

Hassan, M.S., 2018. Moisture sensitivity and dimensional stability of carbonated fibre-cement composites. *Advances in Cement Research*, 30(9), pp.413-426. [Doi:10.1680/jadcr.17.00141](https://doi.org/10.1680/jadcr.17.00141).

Ibrahim, T.H. and Allawi, A.A., 2023. The Response of Reinforced Concrete Composite Beams Reinforced with Pultruded GFRP to Repeated Loads. *Journal of Engineering*, 29(1), pp.158-174. [Doi:10.31026/j.eng.2023.01.10](https://doi.org/10.31026/j.eng.2023.01.10).

Irshidat, M.R. and Al-Saleh, M.H., 2018. Thermal performance and fire resistance of nanoclay modified cementitious materials. *Construction and Building Materials*, 159, pp.213-219. [Doi:10.1016/j.conbuildmat.2017.10.127](https://doi.org/10.1016/j.conbuildmat.2017.10.127).

Janca, M., Siler, P., Opravil, T. and Kotrla, J., 2019, July. Improving the dispersion of silica fume in cement pastes and mortars. In *IOP Conference Series: Materials Science and Engineering* (Vol. 583, No. 1, p. 012022). IOP Publishing. [Doi:10.1088/1757-899X/583/1/012022](https://doi.org/10.1088/1757-899X/583/1/012022).

Joint ACI/TMS Comm 216, 216.1-14, 2019. Code Requirements for Determining Fire Resistance of Concrete and Masonry Construction Assemblies. *American Concrete Institute*, Farmington Hills, MI.

Kattoof, I., Hassan, M.S. and Hasan, S.S., 2022. Effects of liquid nitrogen cooling on the microstructure properties of nano-modified concrete under hot conditions. *Arabian Journal for Science and Engineering*, 47(10), pp.12569-12583. [Doi:10.1007/s13369-021-06496-5](https://doi.org/10.1007/s13369-021-06496-5).

Khalid, M.Q. and Abbas, Z.K., 2023. Producing Sustainable Roller Compacted Concrete by Using Fine Recycled Concrete Aggregate. *Journal of Engineering*, 29(5), pp.126-145. [Doi: 10.31026/j.eng.2023.05.10](https://doi.org/10.31026/j.eng.2023.05.10).

Khaloo, A.R., Vayghan, A.G. and Bolhassani, M., 2011. Mechanical and microstructural properties of cement paste incorporating nano silica particles with various specific surface areas. In *Key*





*Engineering Materials* (Vol. 478, pp. 19-24). Trans Tech Publications Ltd.  
[Doi:10.4028/www.scientific.net/KEM.478.19](https://doi.org/10.4028/www.scientific.net/KEM.478.19).

Khoury, G.A., 1992. Compressive strength of concrete at high temperatures: a reassessment. *Magazine of concrete Research*, 44(161), pp.291-309. [Doi: 10.1680/mac.1992.44.161.291](https://doi.org/10.1680/mac.1992.44.161.291)

Kim, K.Y., Yun, T.S. and Park, K.P., 2013. Evaluation of pore structures and cracking in cement paste exposed to elevated temperatures by X-ray computed tomography. *Cement and Concrete Research*, 50, pp.34-40. [Doi:10.1016/j.cemconres.2013.03.020](https://doi.org/10.1016/j.cemconres.2013.03.020)

Kjellsen, K.O., Monsøy, A., Isachsen, K. and Detwiler, R.J., 2003. Preparation of flat-polished specimens for SEM-backscattered electron imaging and X-ray microanalysis—importance of epoxy impregnation. *Cement and concrete research*, 33(4), pp.611-616. [Doi:10.1016/S0008-8846\(02\)01029-3](https://doi.org/10.1016/S0008-8846(02)01029-3).

Knapen, E. and Van Gemert, D., 2009. Cement hydration and microstructure formation in the presence of water-soluble polymers. *Cement and concrete Research*, 39(1), pp.6-13. [Doi:10.1016/j.cemconres.2008.10.003](https://doi.org/10.1016/j.cemconres.2008.10.003)

Kodur, V., 2014. Properties of concrete at elevated temperatures. *International Scholarly Research Notices*. [Doi:10.1155/2014/468510](https://doi.org/10.1155/2014/468510).

Lea, F.C., 1922. The resistance to fire of concrete and reinforced concrete. *Journal of the Society of Chemical Industry*, 41(18), pp.395R-396R. [Doi:10.1002/jctb.5000411814](https://doi.org/10.1002/jctb.5000411814).

Lea, F.C., 1920. The effect of temperature on some of the properties of materials. *Engineering*, 110(3), pp.293-298.

Li, Y., Tan, K.H. and Yang, E.H., 2019. Synergistic effects of hybrid polypropylene and steel fibers on explosive spalling prevention of ultra-high performance concrete at elevated temperature. *Cement and Concrete Composites*, 96, pp.174-181. [Doi:10.1016/j.cemconcomp.2018.11.009](https://doi.org/10.1016/j.cemconcomp.2018.11.009).

Li, L.G., Huang, Z.H., Zhu, J., Kwan, A.K.H. and Chen, H.Y., 2017. Synergistic effects of micro-silica and nano-silica on strength and microstructure of mortar. *Construction and Building Materials*, 140, pp.229-238. [Doi: 10.1016/j.conbuildmat.2017.02.115](https://doi.org/10.1016/j.conbuildmat.2017.02.115)

Mardani-Aghabaglou, A., Sezer, G.İ. and Ramyar, K., 2014. Comparison of fly ash, silica fume and metakaolin from mechanical properties and durability performance of mortar mixtures view point. *Construction and Building Materials*, 70, pp.17-25. [Doi: 10.1016/j.conbuildmat.2014.07.089](https://doi.org/10.1016/j.conbuildmat.2014.07.089)

Mehta, P.K. and Monteiro, P.J., 2014. *Concrete: microstructure, properties, and materials*. McGraw-Hill Education.

Menéndez, E., Andrade, C. and Vega, L., 2012. Study of dehydration and rehydration processes of portlandite in mature and young cement pastes. *Journal of thermal analysis and calorimetry*, 110(1), pp.443-450. [Doi: 10.1007/s10973-011-2167-4](https://doi.org/10.1007/s10973-011-2167-4)

Moghadam, M.A., Izadifard, R.A., 2020. Effects of zeolite and silica fume substitution on the microstructure and mechanical properties of mortar at high temperatures, *construction and building materials*. 253, p.119206. [Doi:10.1016/j.conbuildmat.2020.119206](https://doi.org/10.1016/j.conbuildmat.2020.119206)



Mohammed, Z.M., Abdulhameed, A.A. and Kazim, H.K., 2022. Effect of Alkali-Activated Natural Pozzolan on Mechanical Properties of Geopolymer Concrete. *Civil and Environmental Engineering*, 18(1), pp.312-320. Doi: [10.2478/cee-2022-0029](https://doi.org/10.2478/cee-2022-0029).

Morsy, M.S., Al-Salloum, Y.A., Abbas, H. and Alsayed, S.H., 2012. Behavior of blended cement mortars containing nano-metakaolin at elevated temperatures. *Construction and Building materials*, 35, pp.900-905. Doi:[10.1016/j.conbuildmat.2012.04.099](https://doi.org/10.1016/j.conbuildmat.2012.04.099).

Neville, A. M., 1995. *Properties of Concrete*, fourth ed., English Language Book Society and Pitman, London.

Orchard, D. F., 1997. The properties of cement and concrete. *Concr. Technol.* 1, 317–328.

Seleem, H.E.H., Rashad, A.M. and Elsokary, T., 2011. Effect of elevated temperature on physico-mechanical properties of blended cement concrete. *Construction and Building Materials*, 25(2), pp.1009-1017. Doi:[10.1016/j.conbuildmat.2010.06.078](https://doi.org/10.1016/j.conbuildmat.2010.06.078).

Sharma, U., Khatri, A. Kanoungo, A., 2014. Use of Micro-silica as Additive to Concrete-state of Art, *International Journal of Civil Engineering Research*. 5 (1), pp. 9-12.

Swamy, R. N., 1986. *Cement replacement materials*: Surrey University Press, Surrey.

Taylor H.F.W., 1964. *The Chemistry of Cements*: vol. I, Academic Press, London.

Temiz, H. and Karakeci, A.Y., 2002. An investigation on microstructure of cement paste containing fly ash and silica fume. *Cement and Concrete Research*, 32(7), pp.1131-1132. Doi: [10.1016/S0008-8846\(02\)00749-4](https://doi.org/10.1016/S0008-8846(02)00749-4)

Wu, Z., Shi, C. and Khayat, K.H., 2016. Influence of silica fume content on microstructure development and bond to steel fiber in ultra-high strength cement-based materials (UHSC). *Cement and Concrete Composites*, 71, pp.97-109. Doi:[10.1016/j.cemconcomp.2016.05.005](https://doi.org/10.1016/j.cemconcomp.2016.05.005).

Mohammed, Z.M., Abdulhameed, A.A. and Kazim, H.K., 2022. Effect of Alkali-Activated Natural Pozzolan on Mechanical Properties of Geopolymer Concrete. *Civil and Environmental Engineering*, 18(1), pp.312-320. Doi: [10.2478/cee-2022-0029](https://doi.org/10.2478/cee-2022-0029).